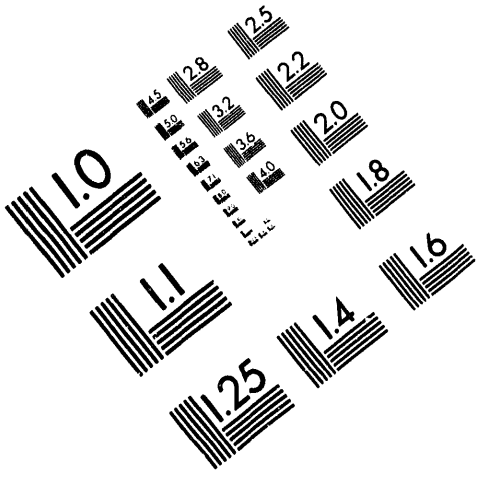

AIIM

Association for Information and Image Management
1100 Wayne Avenue, Suite 1100
Silver Spring, Maryland 20910
301/587-8202

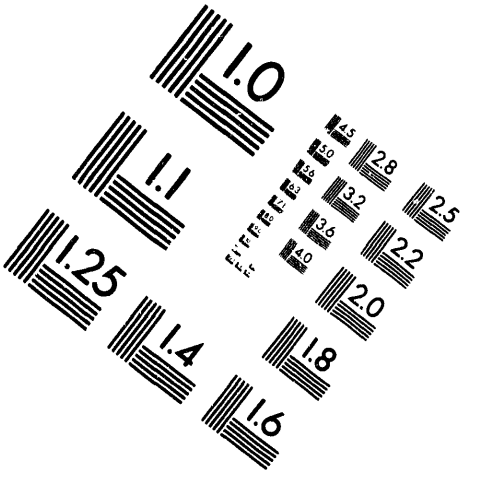

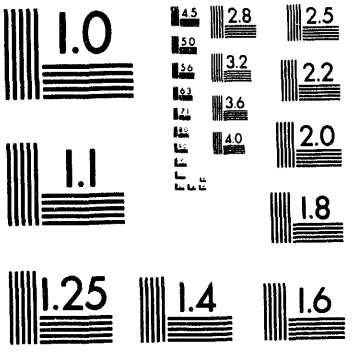

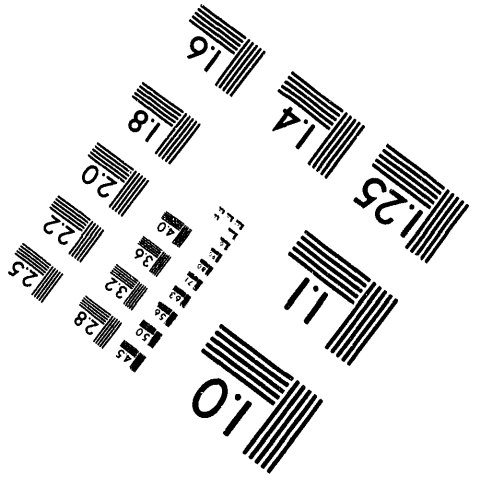

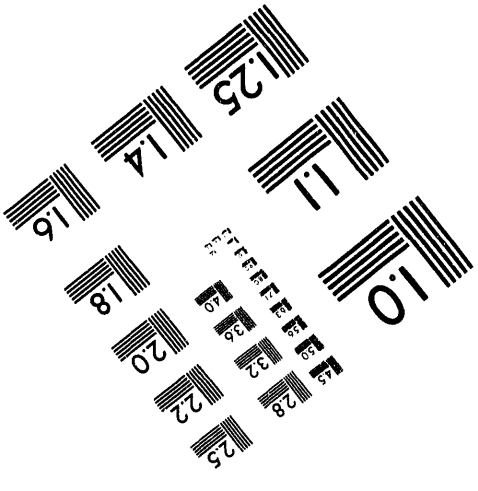

1 of 1

Numerical Simulation of Dynamic Fracture and Failure in Solids

E. P. Chen

Solid and Structural Mechanics Department, Sandia National Laboratories
Albuquerque, New Mexico 87185-0437, U. S. A.

ABSTRACT

Numerical simulation of dynamic fracture and failure processes in solid continua using Lagrangian finite element techniques is the subject of discussion in this investigation. The specific configurations in this study include penetration of steel projectiles into aluminum blocks and concrete slabs. The failure mode in the aluminum block is excessive deformation while the concrete slab fails by hole growth, spallation, and scabbing. The transient dynamic finite element code LS-DYNA2D [1] was used for the numerical analysis. The erosion capability in LS-DYNA2D was exercised to carry out the fracture and failure simulations. Calculated results were compared to the experimental data. Good correlations were obtained.

INTRODUCTION

Advances in mechanics software and computer hardware have led to an ever-increasing reliance on computational simulation to understand complex engineering systems. Lagrangian finite element methods have proven to be versatile tools for simulation of material and structural responses under applied loads. A primary difficulty encountered by numerical analysis techniques is the simulation of material fracture and failure processes wherein mesh separation and excessive mesh distortion problems have to be addressed. One of the simplest methods to simulate fracture and failure numerically is to delete failed elements from further computation in a numerical analysis. An element fails according to a prescribed failure criterion. Difficulties arise when contact surfaces are involved in the problem. The deletion of elements at material interfaces destroys contact surface definitions and results in inaccurate force and momentum transfers. The erosion algorithm deletes elements according to a prescribed failure criterion and rebuilds contact surfaces to maintain interface definitions and allow accurate force and momentum transfers across the interfaces. This paper demonstrates the use of the erosion technique to simulate fracture and failure in solids. The demonstration problems involve steel projectiles impacting aluminum blocks and concrete slabs. The failure mode in the aluminum block is excessive deformation while the concrete slab fails by a combination of deformation-induced hole growth and cracking-induced scabbing and spalling. These problems were selected because they cover both ductile and brittle failure modes and because of the availability of experimental data to verify calculated results.

The erosion technique has been used by several authors [2] for various problems with varying degree of success. As can be expected, the success is highly dependent on the selection of appropriate constitutive model and failure criterion for the material. For the present set of calculations, the aluminum block is modeled as an elastic-plastic, isotropically hardening material. An equivalent plastic strain failure criterion is defined for erosion analysis. The response of the concrete slab in tension is modeled by a micromechanics based damage model. In compression, inelastic concrete response is governed by the pressure-dependent Drucker-Prager model. A tensile fracture criterion based on damage and a compressive failure criterion based on equivalent plastic strain are defined for erosion purposes. The computer code LS-DYNA2D [1] is used to perform the calculations. Good agreements between calculated and measured data are found.

ALUMINUM BLOCK PENETRATION BY A SPHERICAL-NOSE STEEL ROD

Forrestal et al. [3] conducted a series of experiments which consists of spherical-nose projectiles machined from T-200 maraging steel impacting 152 mm diameter 6061-T651 aluminum blocks at velocities ranging from 300 to 1000 m/s. The geometric dimensions of the projectile are 7.11 mm for the nose diameter and 71.12 mm for the length of the cylindrical aft body. In the experiments, the height of the target block was selected based on the impact velocity such that the depth of penetration was less than half of the block height. For a given impact velocity, the height of the block was tabulated in [3]. All tests were conducted in the normal impact configuration. Consequently, the problem is axisymmetric and two-dimensional analysis suffices. Details of the analysis have been given in another publication [4] and will not be repeated here. Only pertinent results will be presented.

Based on the uniaxial compression data [3], 6061-T651 aluminum was modeled in this analysis as an elastic-plastic isotropically hardening solid with a bilinear stress-strain response. In the bilinear model, the Young's modulus is 68.9 GPa, the Poisson's ratio is 0.33, the magnitude of the yield stress is 340 MPa, and the hardening modulus is 25.87 MPa. Post- test observations showed that under the specified impact conditions, the projectile suffered no visible damage for any impact velocity included in the test series. Therefore, the maraging steel projectile is treated as an elastic material with a Young's modulus of 200.0 GPa and a Poisson's ratio of 0.32. A Coulomb friction law is also assumed between steel and aluminum. The coefficient of friction was taken as 0.1 [3]. Based on the parametric studies in [4], the critical equivalent plastic strain value for erosion was fixed at 3.25.

Figure 1 shows a deformed mesh plot of a steel projectile penetrating an aluminum block at 359 m/s impact velocity. Because of symmetry, only half of the geometry has been included in the actual computation. Figure 1 shows a finite element model which consists of 3890 quadrilateral elements and 4067 nodes. At other impact velocities, similar finite element models are used with various target block heights from [3]. The figure is a snapshot of the results of calculations from LS-DYNA2D at 140 microseconds after impact. The projectile remained intact and deformations in the target concentrated around the projectile/target interface. At 140 microseconds after impact, the projectile stopped penetrating and began to rebound. The maximum downward displacement is taken as the depth of penetration. Thus, the calculated depth of penetration for 359 m/s impact velocity is 2.35 cm. At other impact velocities, similar results are obtained. These results are shown in Figure 2 where the penetration depth is plotted versus the impact velocity. Also shown in the figure are measured data from [3]. Good agreement between calculated and measured data is observed.

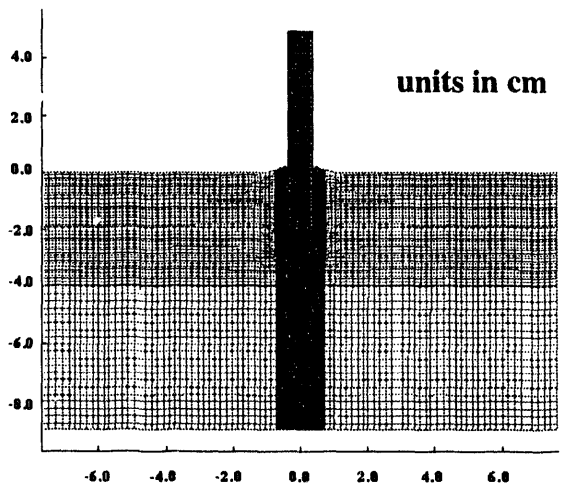

Figure 1. Deformed Mesh at 140 μs.

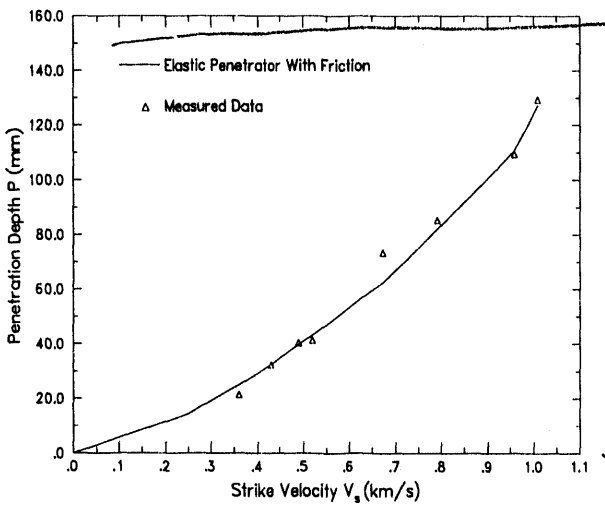

Figure 2. Calculated and Measured Data Comparison.

CONCRETE SLAB PERFORATION BY A STEEL PROJECTILE

Hanchak et. al [5] performed experiments in which 25.4 mm diameter, 143.7 mm long, 0.5 kg, 3.0 caliber-radius-head ogival nose maraging steel projectiles impacted 610x610x178 mm reinforced concrete slabs at velocities between 300 and 1000 m/s. Post-test observations showed that craters were formed at the top and bottom surface while a tunneling phase existed at the middle of the target slab. Also, the steel projectile was observed to sustain little or no damage. Numerical simulation of this series of experiments was performed by Chen [2] in which the concrete was modeled by the soil and crushable foam material model [1]. The soil and crushable foam model decouples the volumetric and deviatoric response of the material. The deviatoric response is elastic-perfectly plastic with a pressure dependent yield surface. The volumetric response allows nonlinear compaction with failure defined by a tensile pressure-cutoff. Although good agreements between calculated and measured data were obtained [2], questions were raised about the lack of specific fracture mechanism and strain-rate effect inherent in the soil and crushable foam model. In an attempt to address these two issues, this paper presents the numerical simulation of the experiments [5] in which concrete is modeled by a strain-rate dependent continuum damage model [6].

The basic assumption of the continuum damage model [6] is that the material is permeated by an array of randomly distributed cracks which grow and interact with one another under tensile loads. The model does not treat each individual crack, but rather treats the growth and interaction of cracks as an internal state variable which represents the accumulation of damage in the material. This damage is assumed to degrade material stiffness following the expressions of Budiansky and O'Connell for a random array of penny-shaped cracks in an isotropic elastic medium. The crack density is expressed as a Weibull statistical distribution activated by volumetric strain. The model is explicitly strain-rate dependent in that the characteristic dimension of the cracks is determined from a dynamic fragmentation expression [6] and that model constants are obtained from rate-dependent fracture stress data. In compression, the material is assumed to behave as a pressure-dependent Drucker-Prager solid. No hardening is considered. This is an improvement from the original damage model developed by Taylor et. al [7] where the compressional response is elastic-perfectly plastic. Triaxial data were obtained in [5] and strain-rate dependent fracture stress data can be estimated from the expression in [7] derived from fracture mechanics. Thus, the concrete has a density of 2.52 g/cm^3, a Young's modulus of 20.68 GPa, a Poisson's ratio of 0.18, a pressure-dependent shear strength of τ=220.8+0.313p (MPa), and a fracture toughness of 2.747 MPa-m$^{1/2}$. The power m and constant k from the Weibull expression are estimated as 6.0 and 5.753x10^{21} m^{-3}, respectively. Critical values for erosion based on damage and equivalent plastic strain are set at 0.5 and 2.5. The steel projectile is elastic with density of 8.02 g/cm^3, a Young's modulus of 206.9 GPa, and a Poisson's ratio of 0.3. Coulomb friction coefficient between steel and concrete is taken as 0.08.

Figure 3 shows a deformed mesh plot of a steel projectile penetrating into a concrete slab at 587 m/s impact velocity, focusing on areas near the center of the slab at 500 microsecond after impact. Axisymmetry is assumed and the actual calculation uses only half of the geometry shown in Figure 3. The calculational mesh contains 9103 quadrilateral elements and 9350 nodes. At other impact velocities, response similar to that in Figure 3 is obtained. Observed qualitative features such as top and bottom surface spallation and middle slab hole growth are duplicated in the numerical simulations. Comparison between measured and calculated results in terms of residual projectile velocity versus strike velocity plot is given in Figure 4. For the range of impact velocity included, good agreement between calculated and measured data has been obtained.

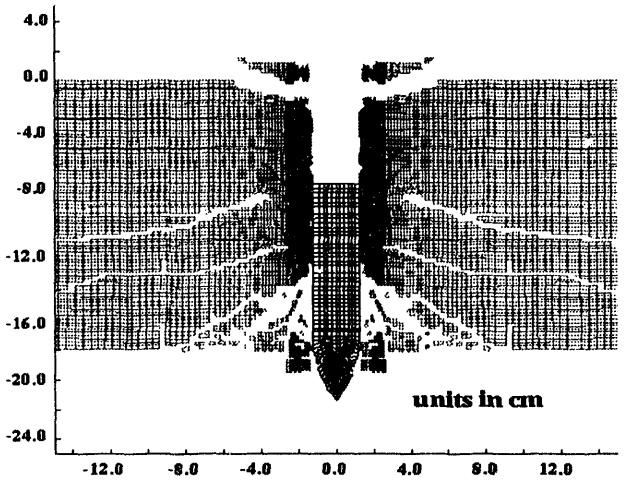

Figure 3. Deformed mesh plot for concrete perforation case.

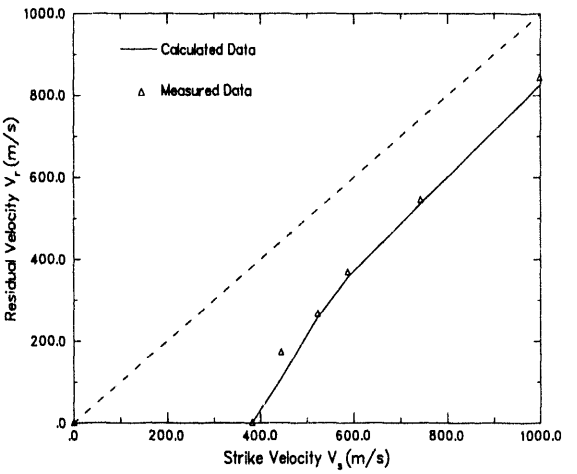

Figure 4. Data comparison for concrete perforation case.

SUMMARY

Numerical simulations of the dynamic fracture and failure of solids are presented in terms of penetration and perforation of aluminum blocks and concrete slabs by steel projectiles. Numerical failure and fracture simulation are achieved by utilizing the erosion algorithm to delete elements and rebuild contact surfaces. Comparisons between calculated and measured data were made. For the range of materials and impact velocities included, good agreements between calculated and measured results were found.

ACKNOWLEGEMENT

This work was funded by the Laboratory Directed Research and Development Program, Sandia National Laboratories, under the auspices of the U. S. Department of Energy under Contract Number DE-AC04-94AL85000.

REFERENCES

[1] Hallquist, J. O., "LS-DYNA2D, an explicit two-dimensional hydrodynamic finite element code," Livermore Software Technology Corporation, Livermore, California, 1990.

[2] Chen, E. P. and Luk, V. K., Editors, *Advances in Numerical Simulation Techniques for Penetration and Perforation of Solids*, AMD-Vol. 171, American Society of Mechanical Engineers, 1993.

[3] Forrestal, M. J., Brar, N. S., and Luk, V. K., "Penetration of strain-hardening targets with rigid spherical-nose rods," Journal of Applied Mechanics, Vol. 58, No. 1, pp. 7-10, 1991.

[4] Chen, E. P., "Numerical simulation of penetration of aluminum targets by spherical-nose steel rods," submitted for publication.

[5] Hanchak, S. J., Forrestal, M. J., Young, E. R., and Ehrgott, J. Q., "Perforation of concrete slabs with 48 MPa and 140 MPa unconfined compressive strengths," International Journal of Impact Engineering, Vol. 12, pp. 1-7, 1992.

[6] Chen, Z. and Chen, E. P., "A vectorized coupled damage/plasticity model for rate-dependent rocks," submitted for publication.

[7] Taylor, L. M., Chen, E. P., and Kuszmaul, J. S., "Microcrack-induced damage accumulation in brittle rock under dynamic loading," Journal of Computer Methods in Applied Mechanics and Engineering, Vol. 55, pp. 301-320, 1986.

DATE
FILMED
6/14/94

END